

Supporting Information

Dynamic Interactions of Fully Glycosylated SARS-CoV-2 Spike Protein with Various Antibodies

Yiwei Cao¹, Yeol Kyo Choi¹, Martin Frank², Hyeonuk Woo³, Sang-Jun Park¹, Min Sun Yeom⁴,
Chaok Seok³, and Wonpil Im^{1*}

¹Departments of Biological Sciences, Chemistry, Bioengineering, and Computer Science and Engineering, Lehigh University, Bethlehem, Pennsylvania 18015, USA

²Biognos AB, Box 8963, 40274 Göteborg, Sweden

³Department of Chemistry, Seoul National University, Seoul 08826, Republic of Korea

⁴Korean Institute of Science and Technology Information, Daejeon 34141, Republic of Korea

*Corresponding authors: wonpil@lehigh.edu

Table S1. Glycosylation sites, selected glycan compositions, and glycan sequences in this study.

Site	Composition and Type	Sequence
N61 N122 N603 N709 N717 N801 N1074	HexNAc(2)Hex(5) High-Mannose	
N234	HexNAc(2)Hex(8) High-Mannose	
N657	HexNAc(3)Hex(6) Hybrid	
N149 N331 N343 N616 N1134	HexNAc(4)Hex(3) Fuc(1) Complex	
N1098 ¹	HexNAc(4)Hex(4) Fuc(1)NeuAc(1) Complex	
N165 ¹	HexNAc(4)Hex(5) Fuc(3)NeuAc(1) Complex	
N282	HexNAc(5)Hex(3) Fuc(1) Complex	
N17 ²	HexNAc(5)Hex(4) Fuc(1) Complex	
N74 ³	HexNAc(6)Hex(4) Fuc(1)NeuAc(1) Complex	
T323	O-glycan	

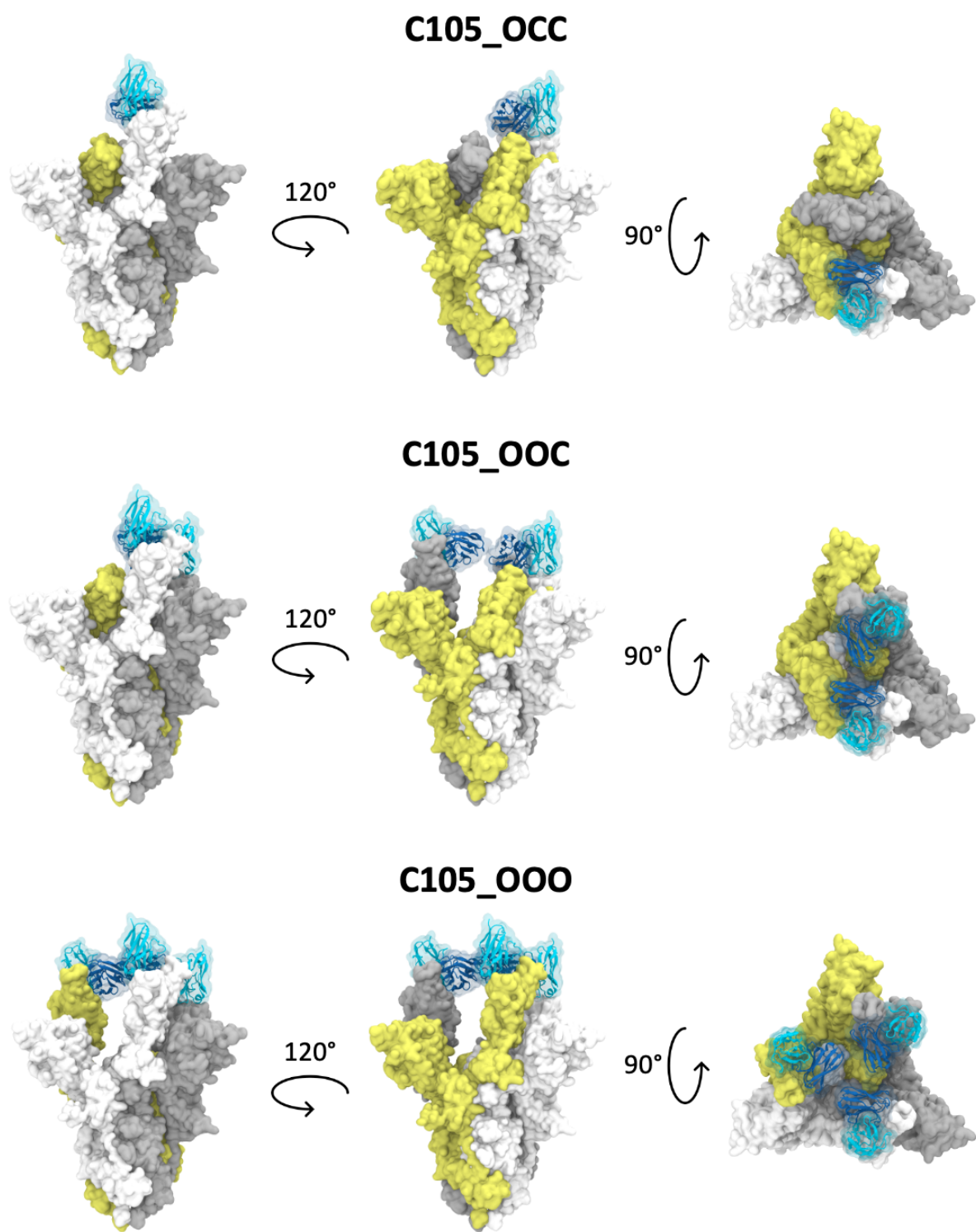
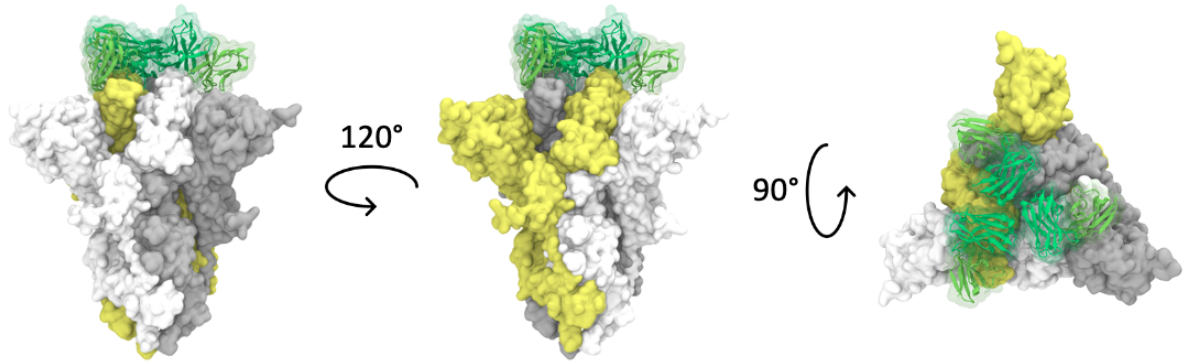
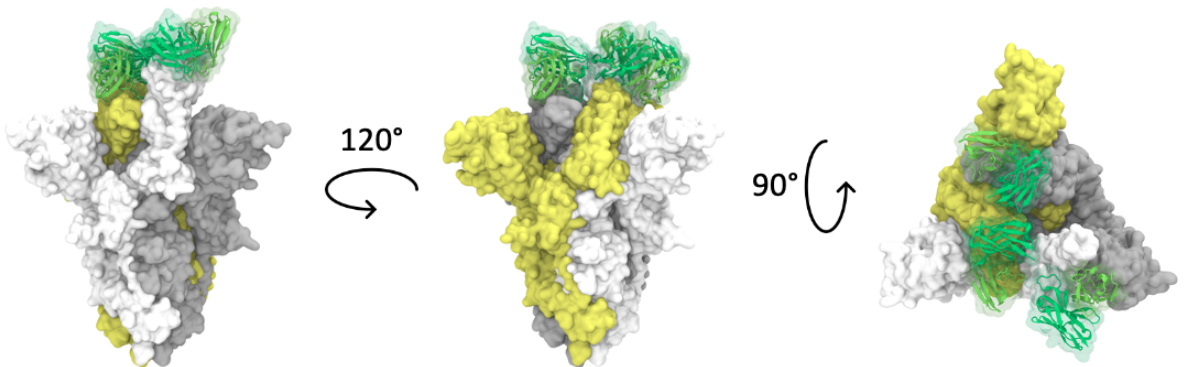


Figure S1. Illustration of C105_OCC, C105_OOC and C105_OOO. The three protomers of S protein are shown in white, gray, and yellow respectively, and the antibodies are shown in blue.

C119_CCC



C119_OCC



C119_OOC

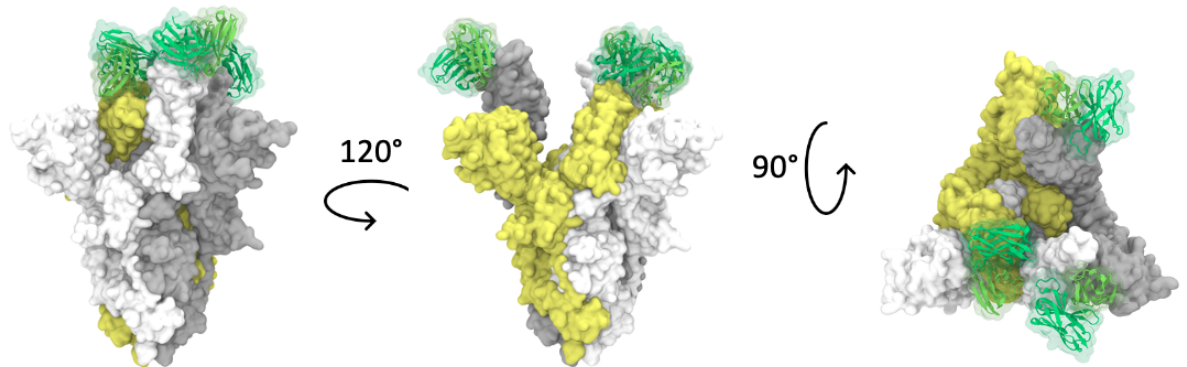
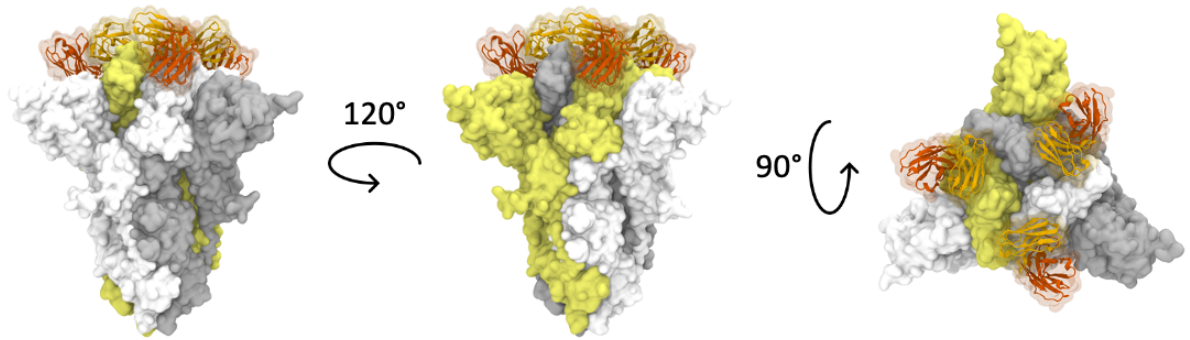


Figure S2. Illustration of C119_CCC, C119_OCC and C119_OOC. The three protomers of S protein are shown in white, gray, and yellow respectively, and the antibodies are shown in green.

S309_CCC



S309_OCC

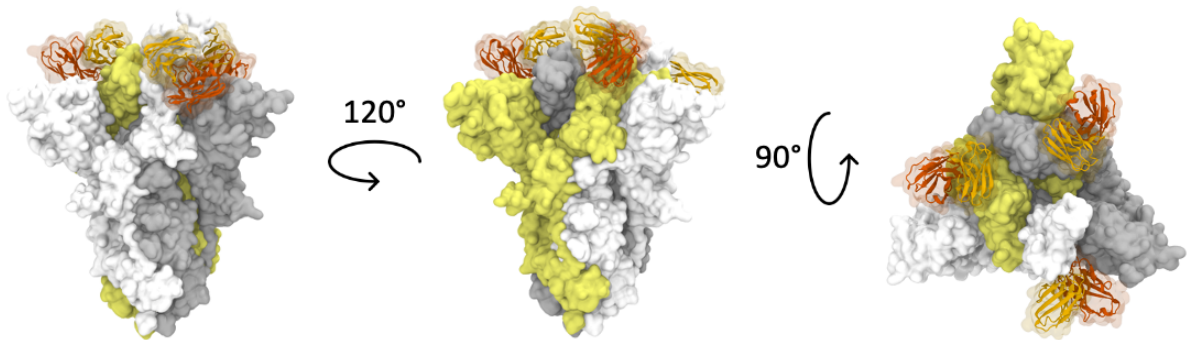


Figure S3. Illustration of S309_CCC, and S309_OCC. The three protomers of S protein are shown in white, gray, and yellow respectively, and the antibodies are shown in orange.

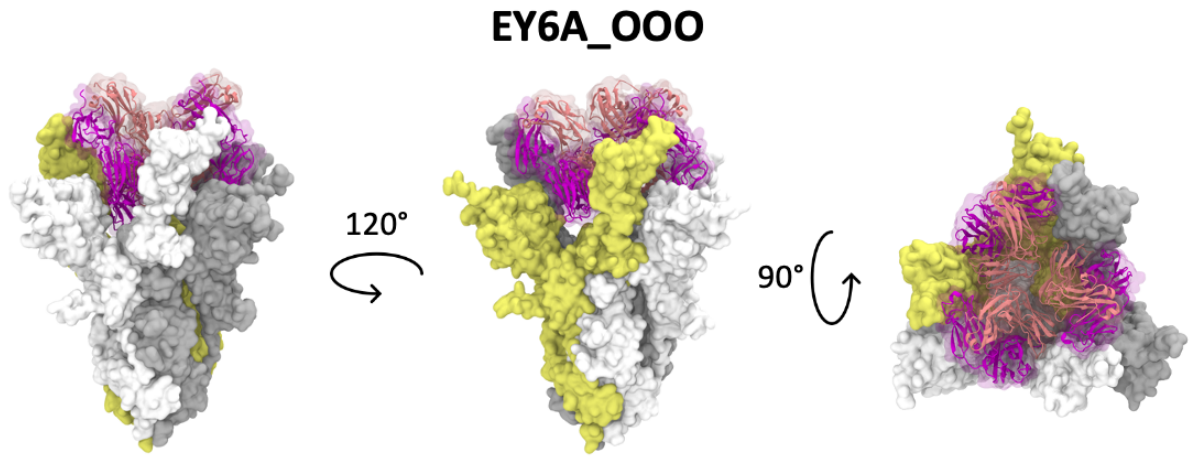


Figure S4. Illustration of EY6A_OOO. The three protomers of S protein are shown in white, gray, and yellow respectively, and the antibodies are shown in magenta.

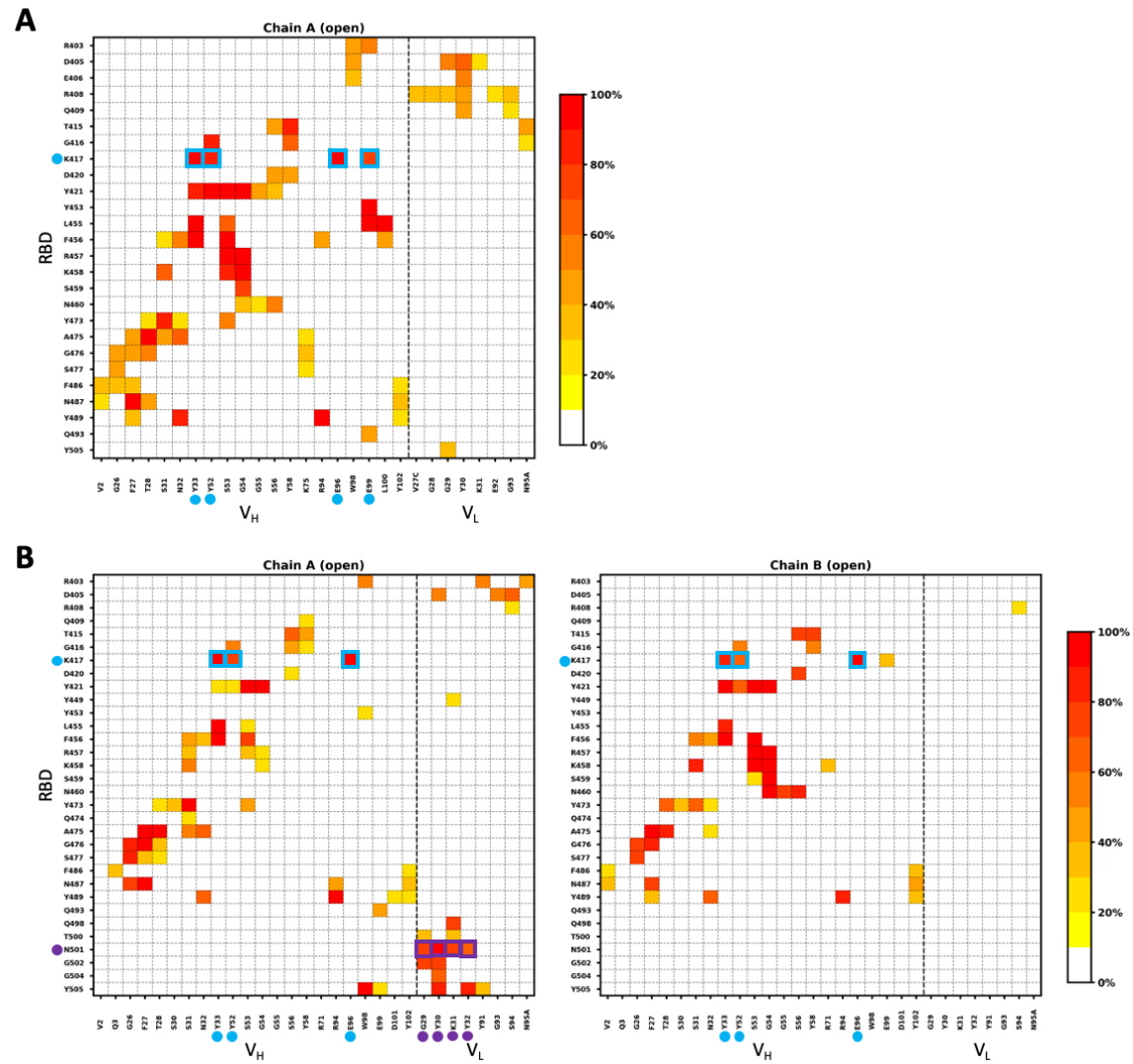


Figure S5. The frequency of interacting residue pairs in C105 systems. (A) C105_OCC, (B) C105_OOC, and (C) C105_OOO.

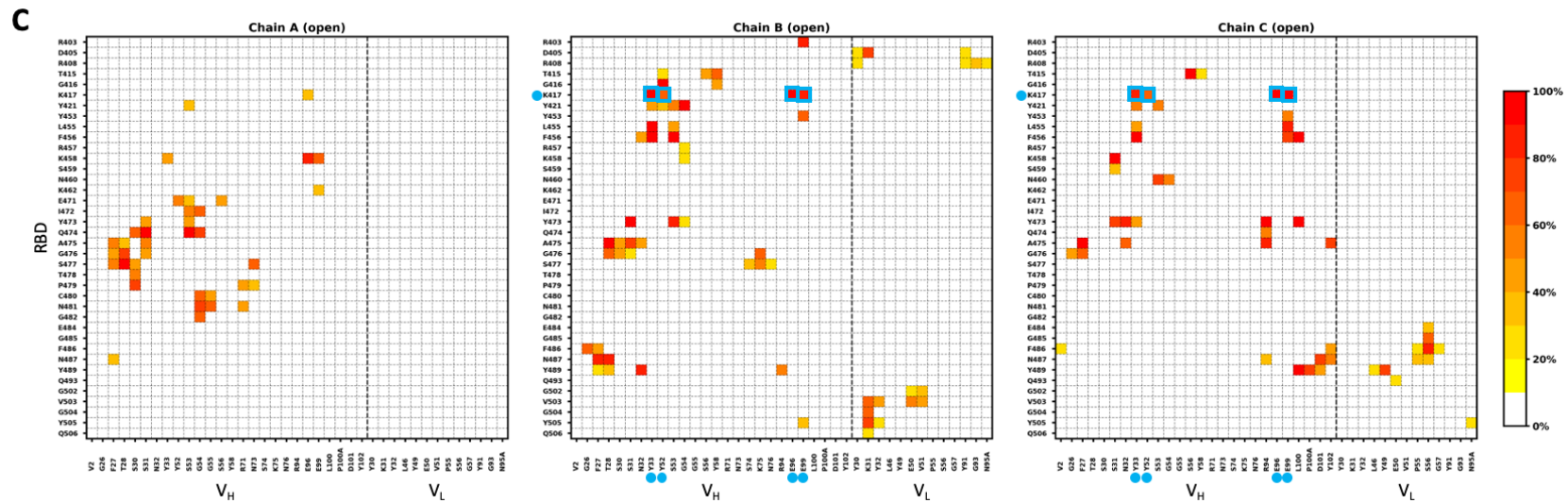


Figure S5 (Continued). The frequency of interacting residue pairs in C105 systems. (A) C105_OCC, (B) C105_OOC, and (C) C105_OOO.

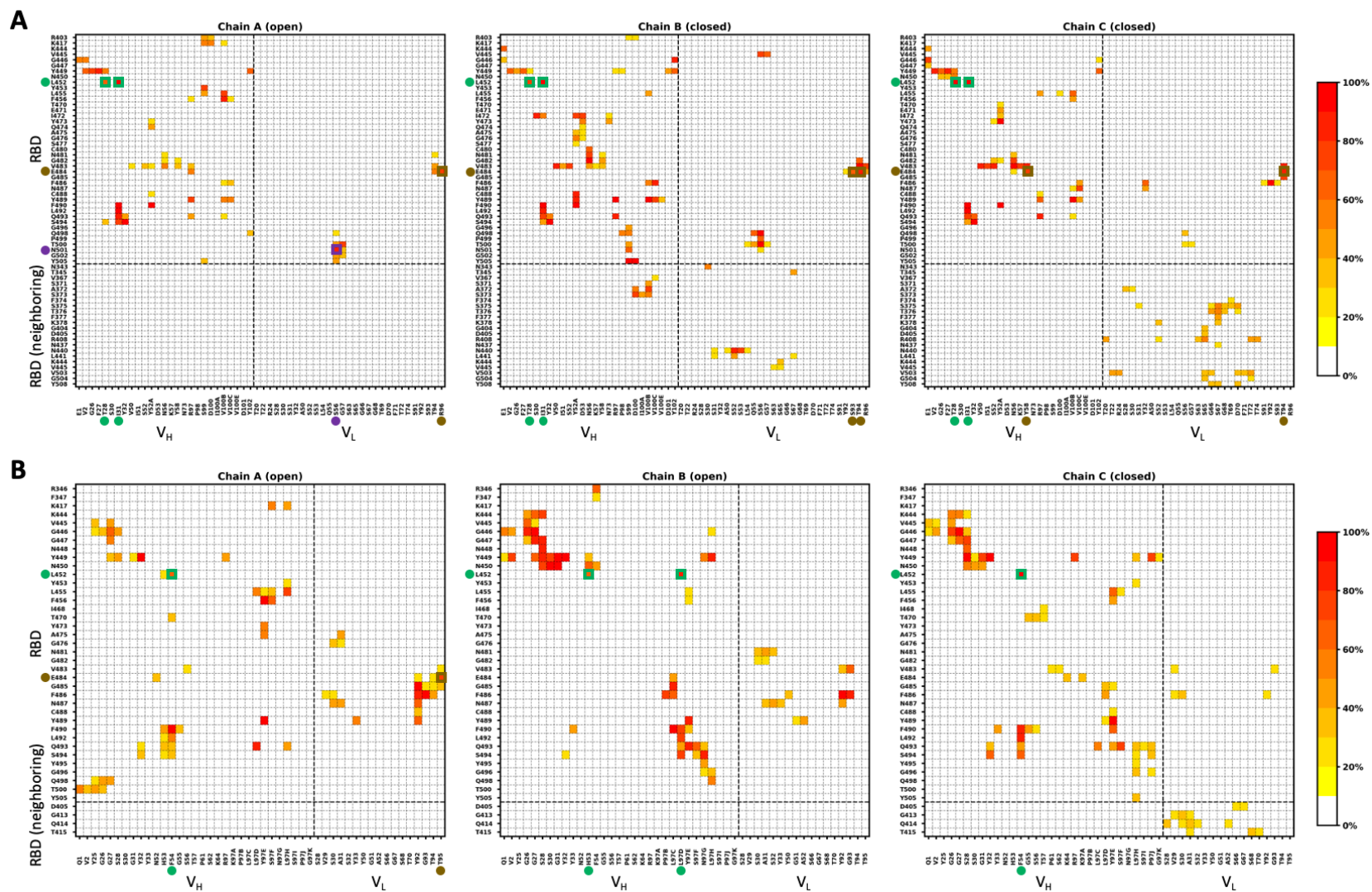


Figure S6. The frequency of interacting residue pairs in C002 systems. (A) C002_OCC and (B) C002_OOC.

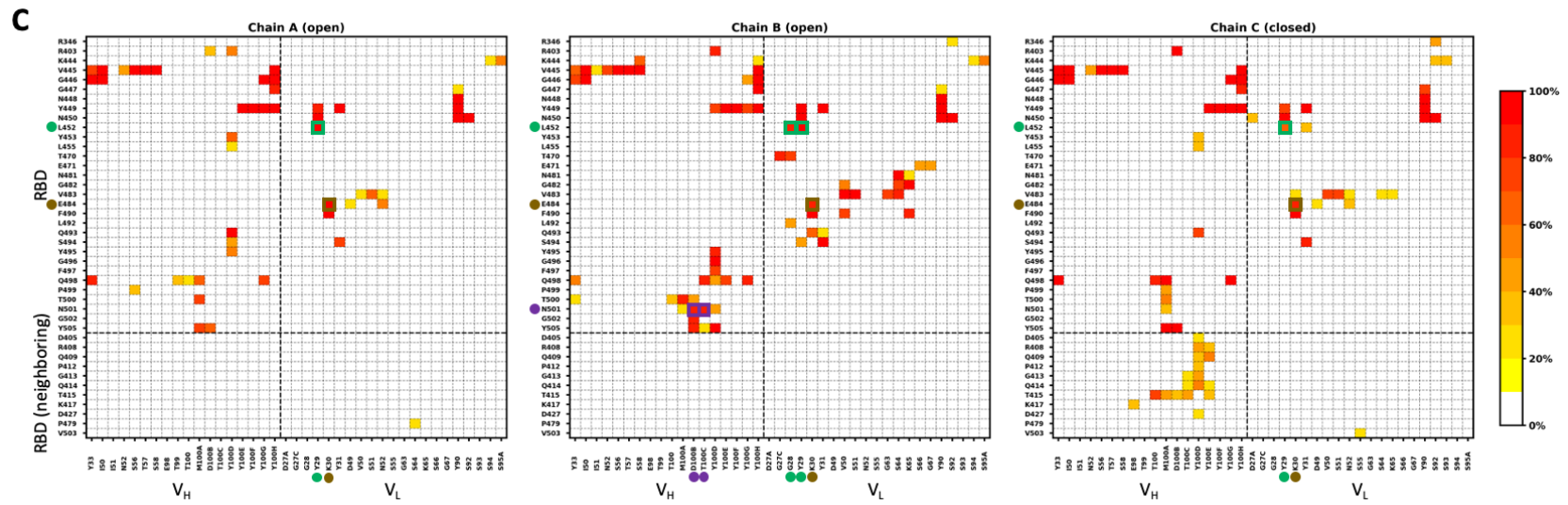


Figure S7 (Continued). The frequency of interacting residue pairs in C119 systems. (A) C119_CCC, (B) C119_OCC, and (C) C119_OOC.

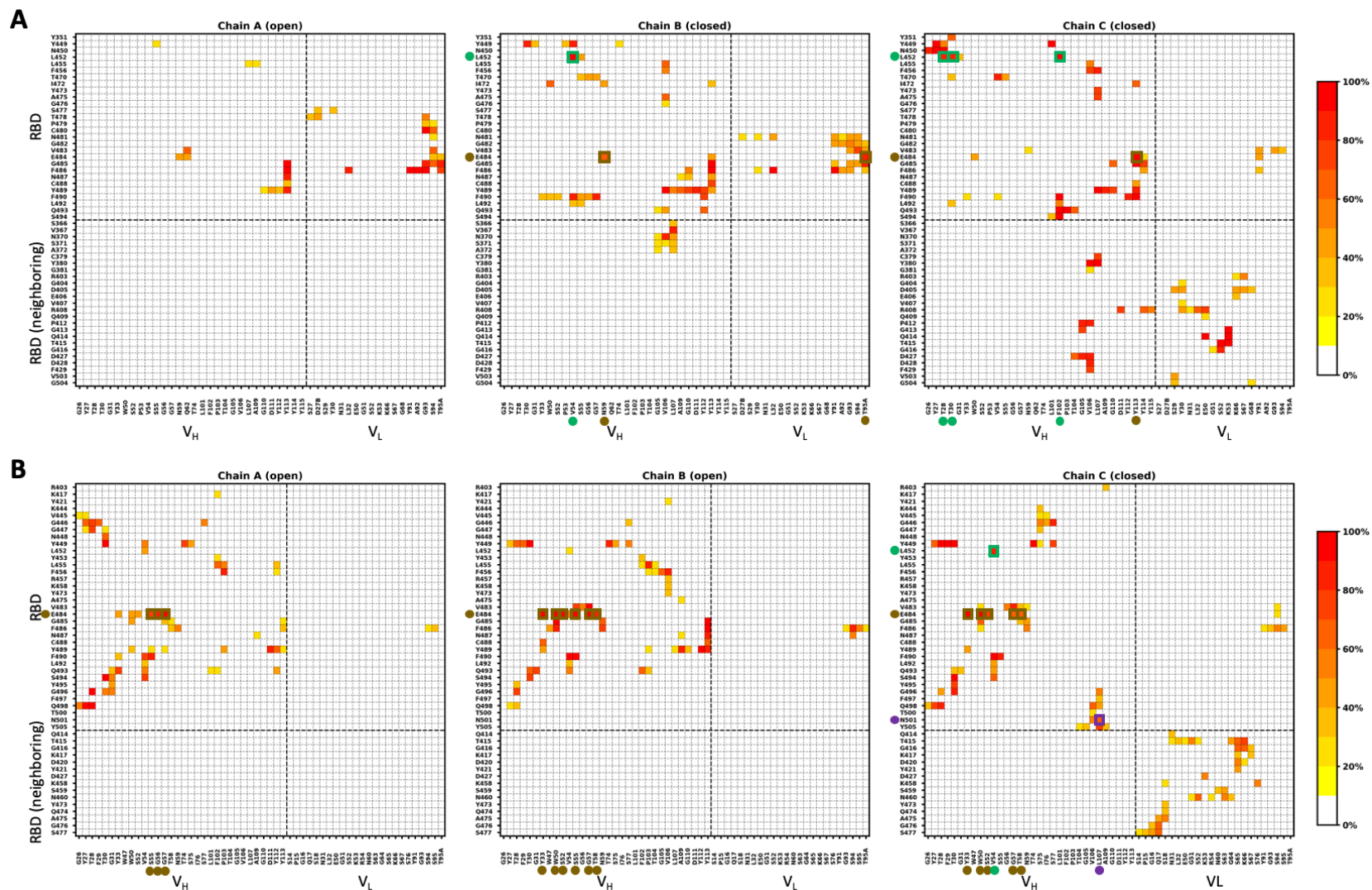


Figure S8. The frequency of interacting residue pairs in C121 systems. (A) C121_OCC and (B) C121_OOC.

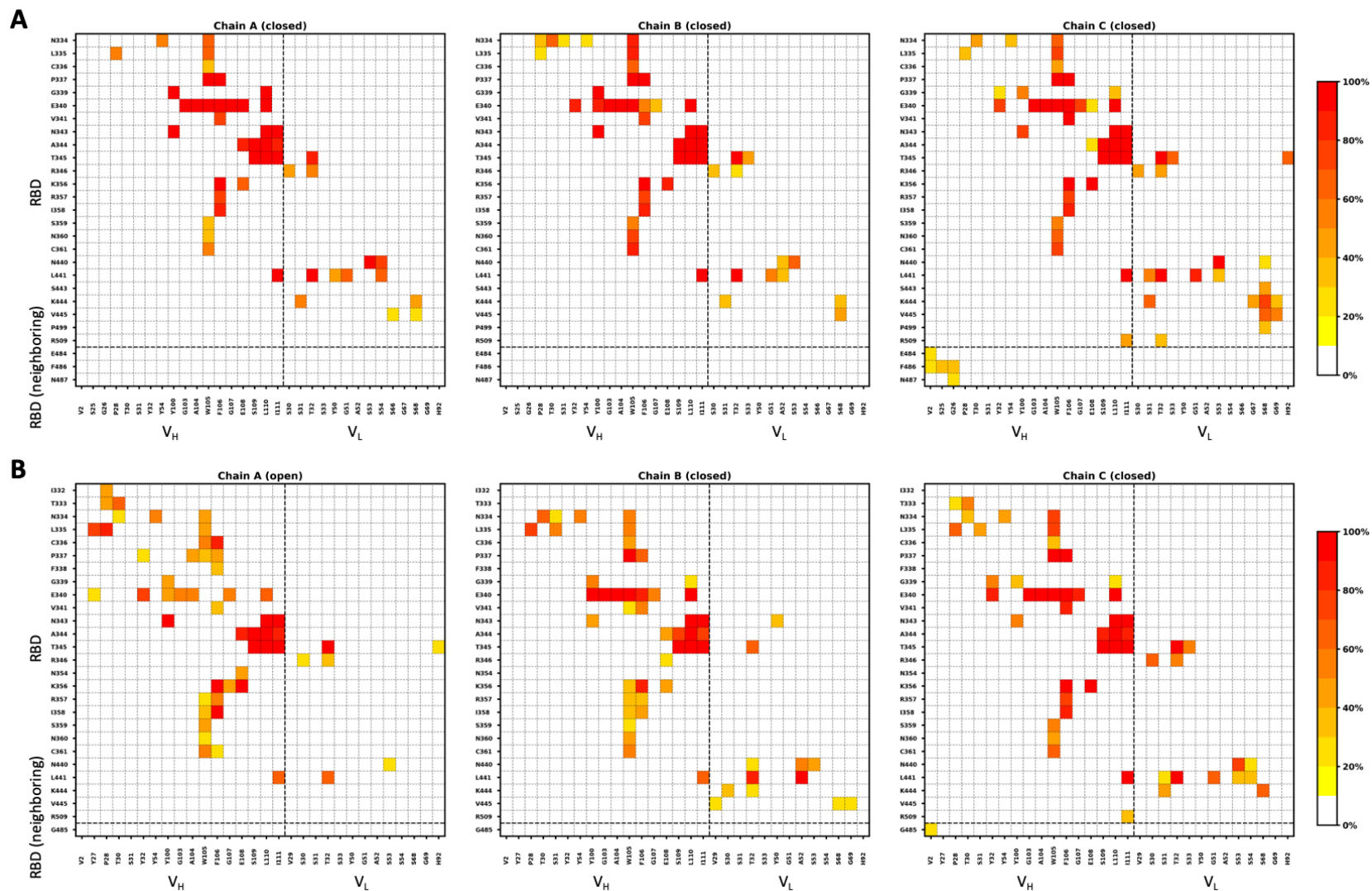


Figure S9. The frequency of interacting residue pairs in S309 systems. (A) S309_CCC and (B) S309_OCC.

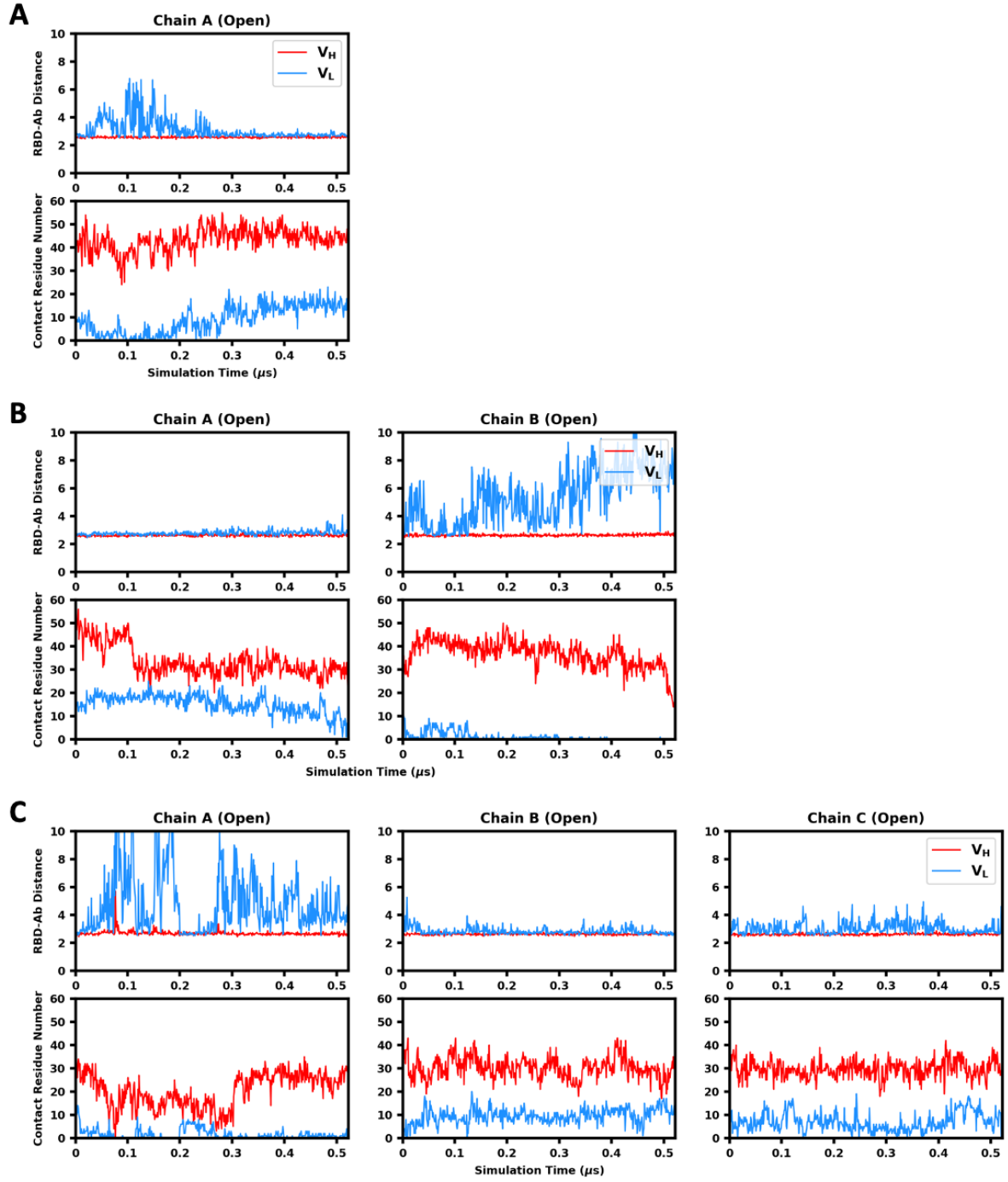


Figure S11. RBD-antibody distance and contact residue number in C105 systems. (A) C105_OCC, (B) C105_OOC, and (C) C105_OOO.

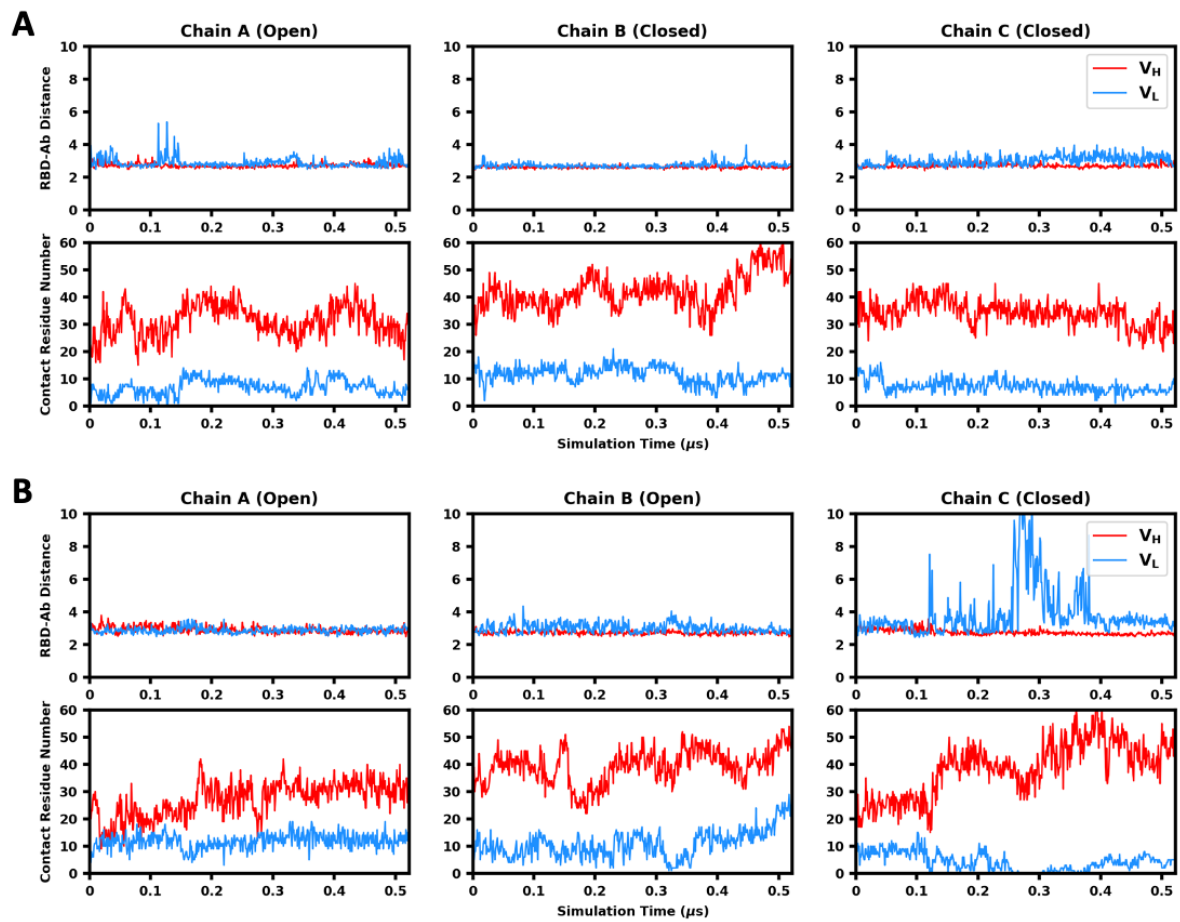


Figure S12. RBD-antibody distance and contact residue number in C002 systems. (A) C002_OCC and (B) C002_OOC.

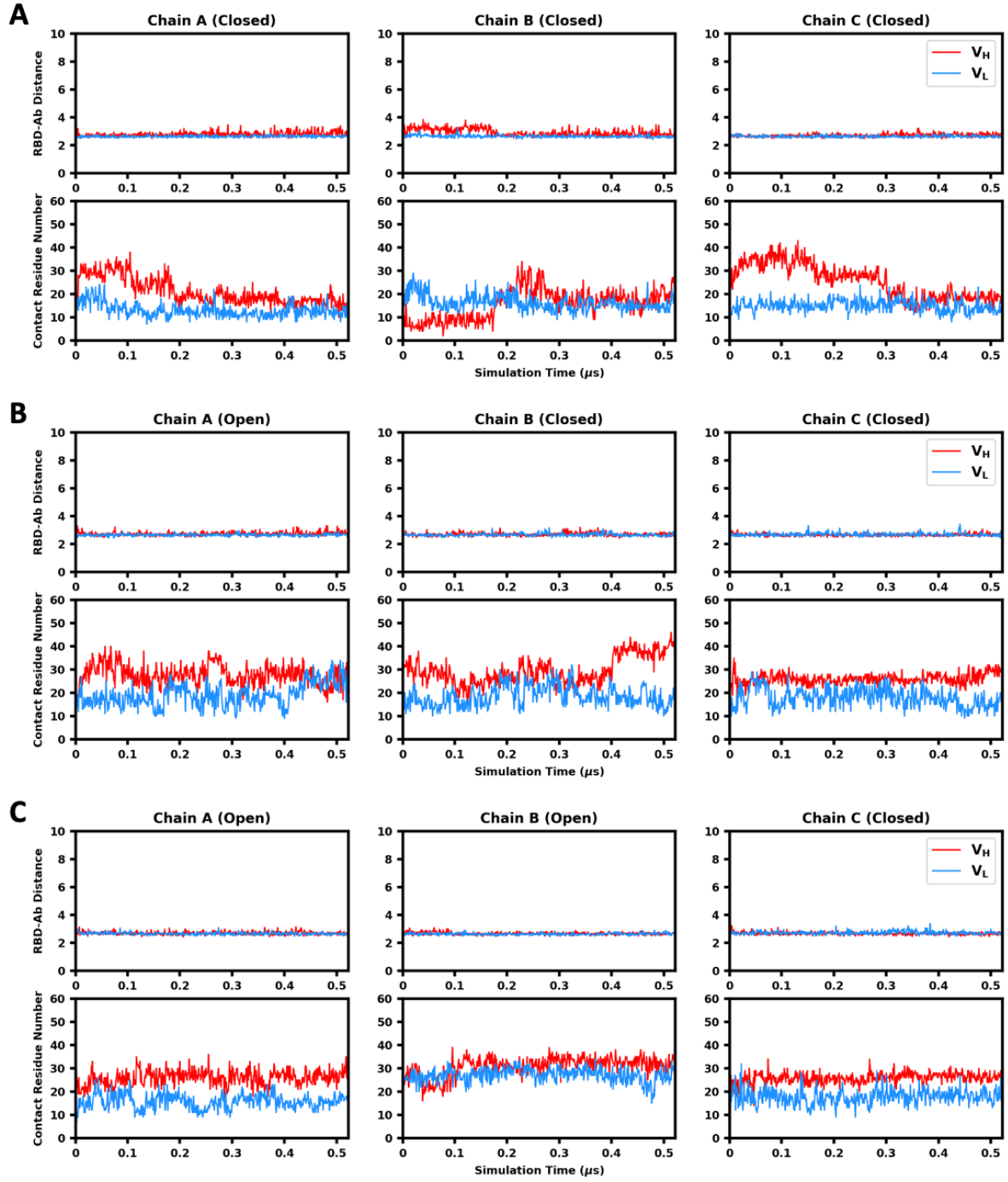


Figure S13. RBD-antibody distance and contact residue number in C119 systems. (A) C119_CCC, (B) C119_OCC, and (C) C119_OOC.

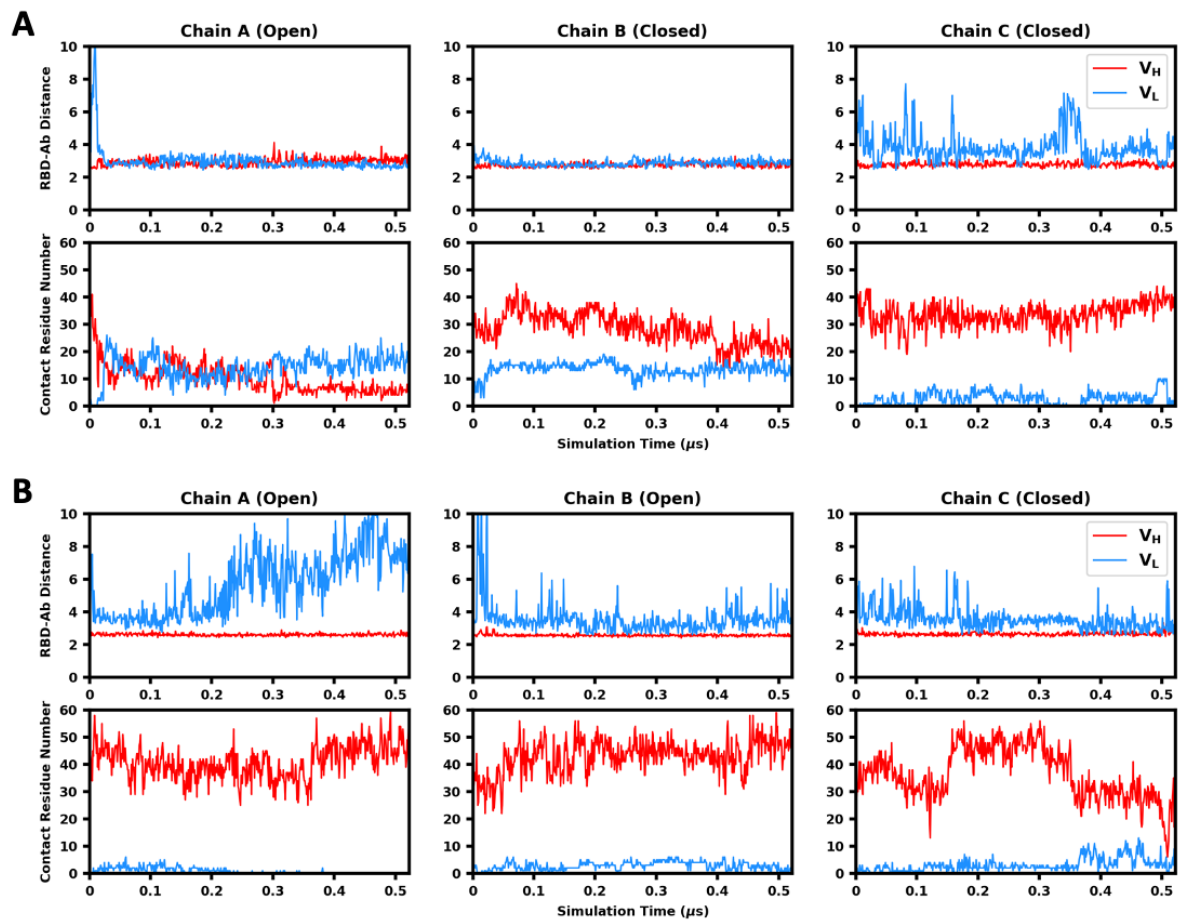


Figure S14. RBD-antibody distance and contact residue number in C121 systems. (A) C121_OCC and (B) C121_OOC.

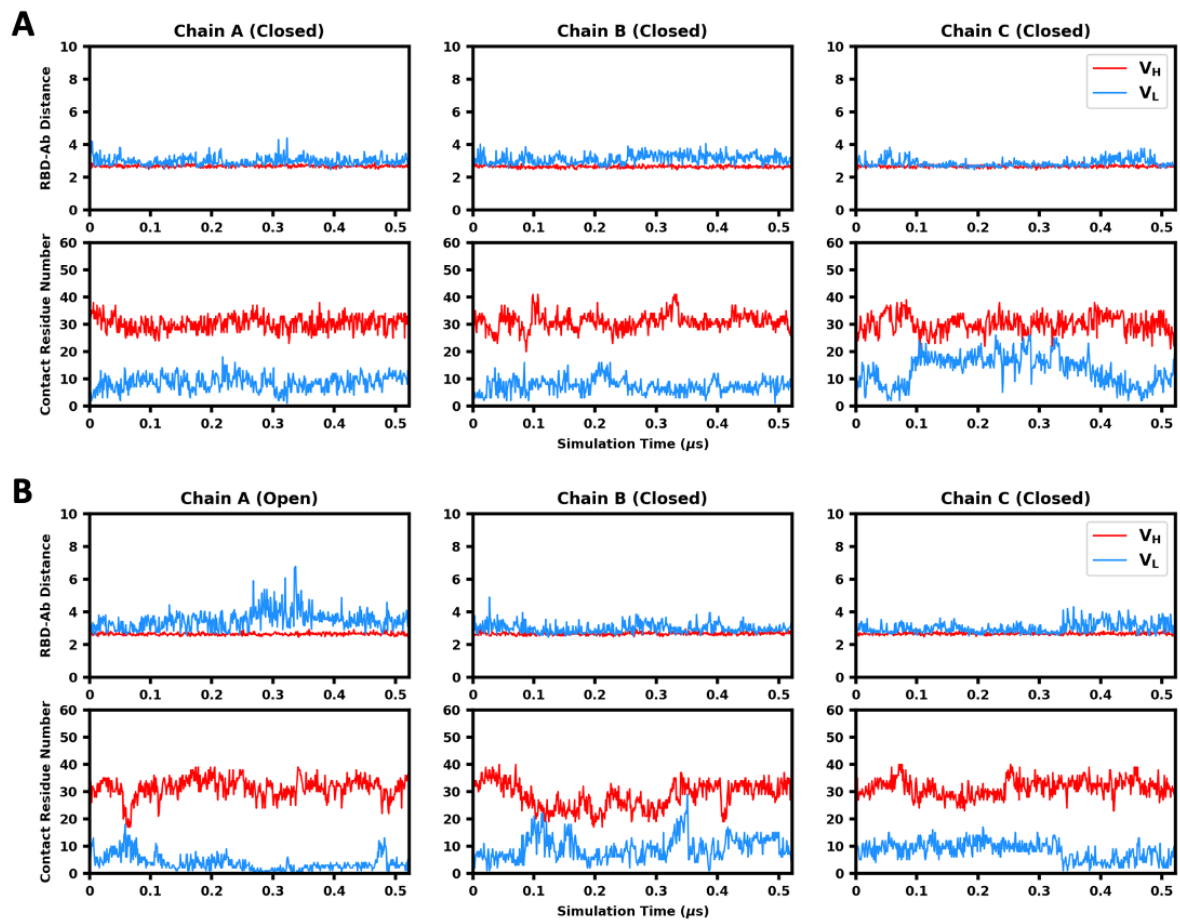


Figure S15. RBD-antibody distance and contact residue number in S309 systems. (A) S309_CCC and (B) S309_OCC.

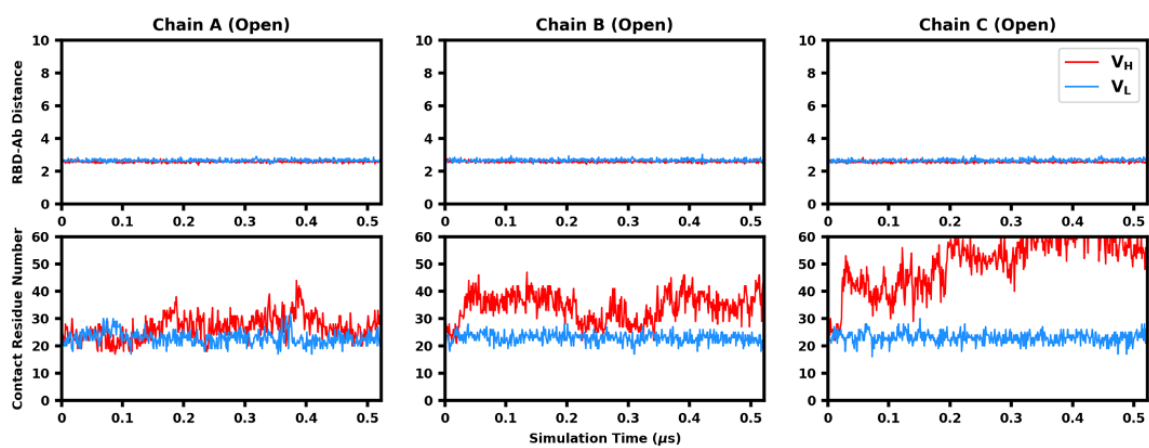


Figure S16. RBD-antibody distance and contact residue number in EY6A_OOO.

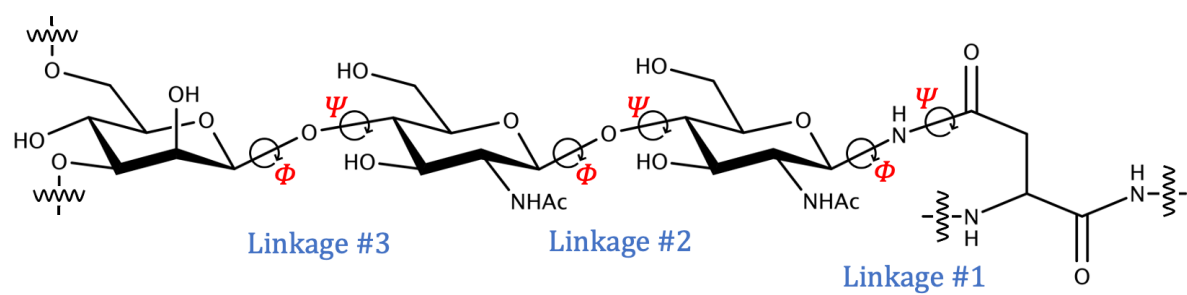


Figure S17. Illustration of ϕ/ψ angles in the first three glycosidic linkages from the reducing terminus.

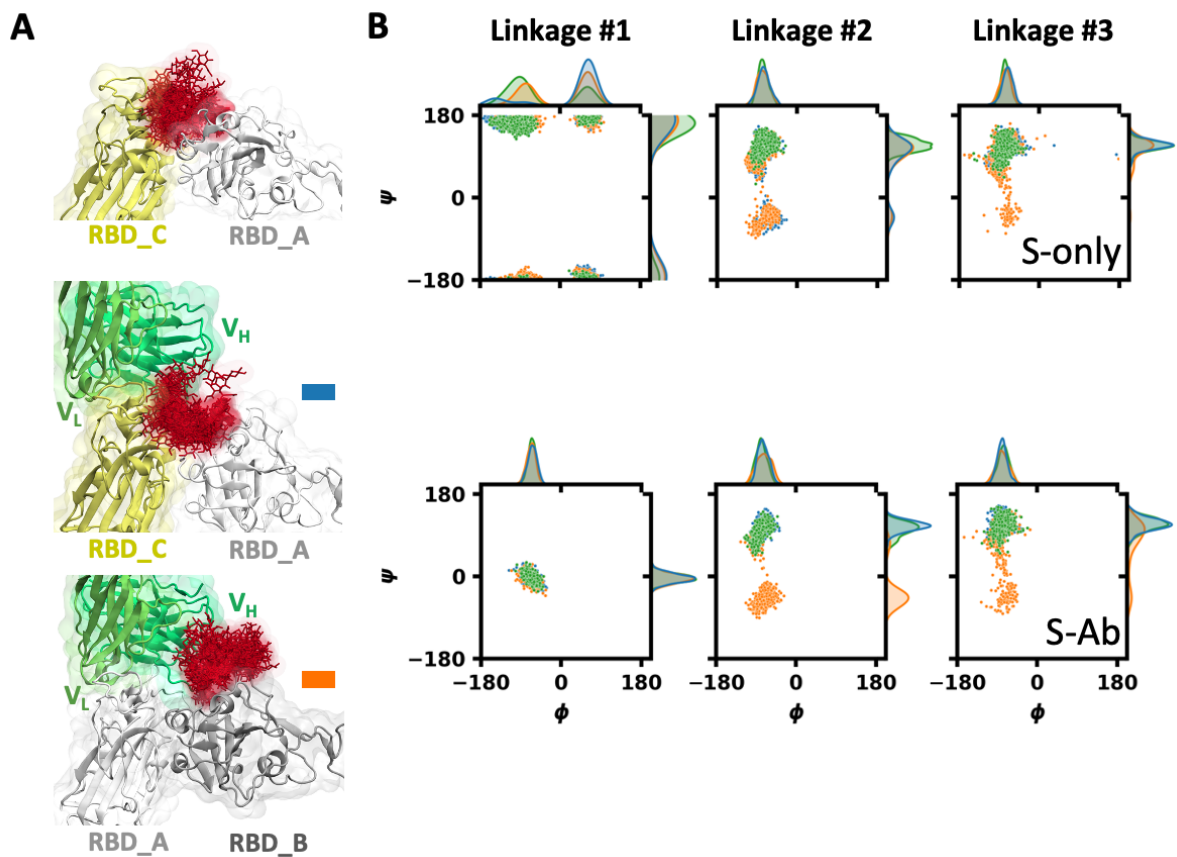


Figure S19. Glycan flexibility in S-only and S-antibody complex systems: N343 glycan in C119_CCC. (A) The structures generated by superimposing the glycan (red) onto the initial structure. (B) The distributions of ϕ/ψ angles in the first three glycosidic linkages from the reducing terminus (see **Figure S17**). The glycans attached to three protomers (chains A, B, and C) are shown in blue, orange, and green, respectively. For S-antibody complex systems, we show the structures of N343 glycan attached to RBD_A (blue) and RBD_B (orange), where the glycan is sampled on two different neighbors.

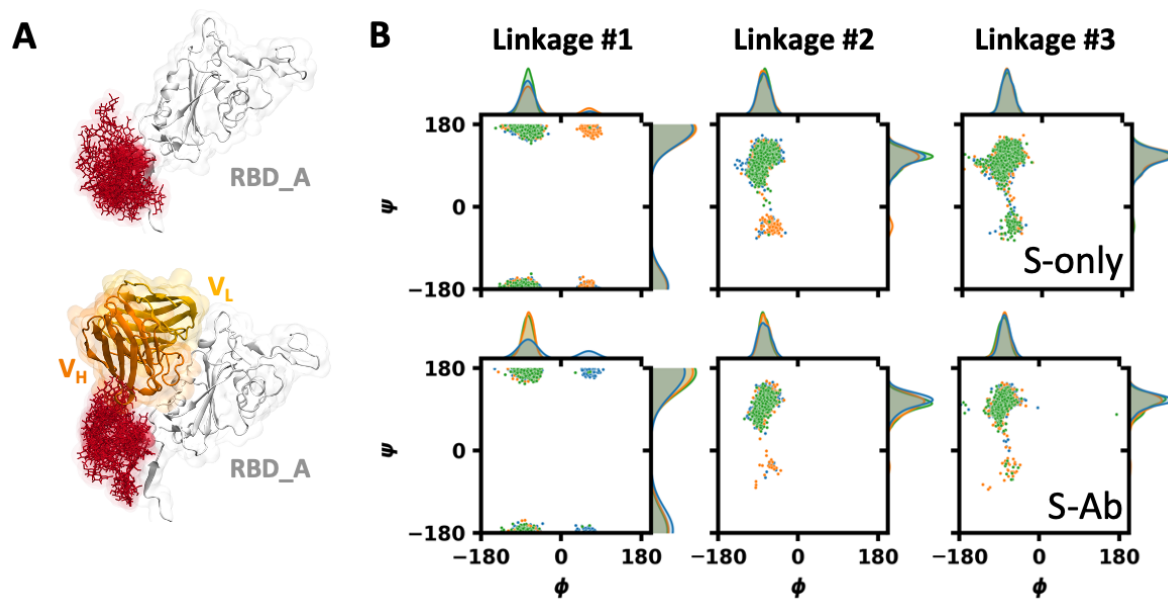


Figure S20. Glycan flexibility in S-only and S-antibody complex systems: N331 glycan in S309_CCC. (A) The structures generated by superimposing the glycan (red) onto the initial structure. (B) The distributions of ϕ/ψ angles in the first three glycosidic linkages from the reducing terminus. The glycans attached to three protomers (chains A, B, and C) are shown in blue, orange, and green, respectively.

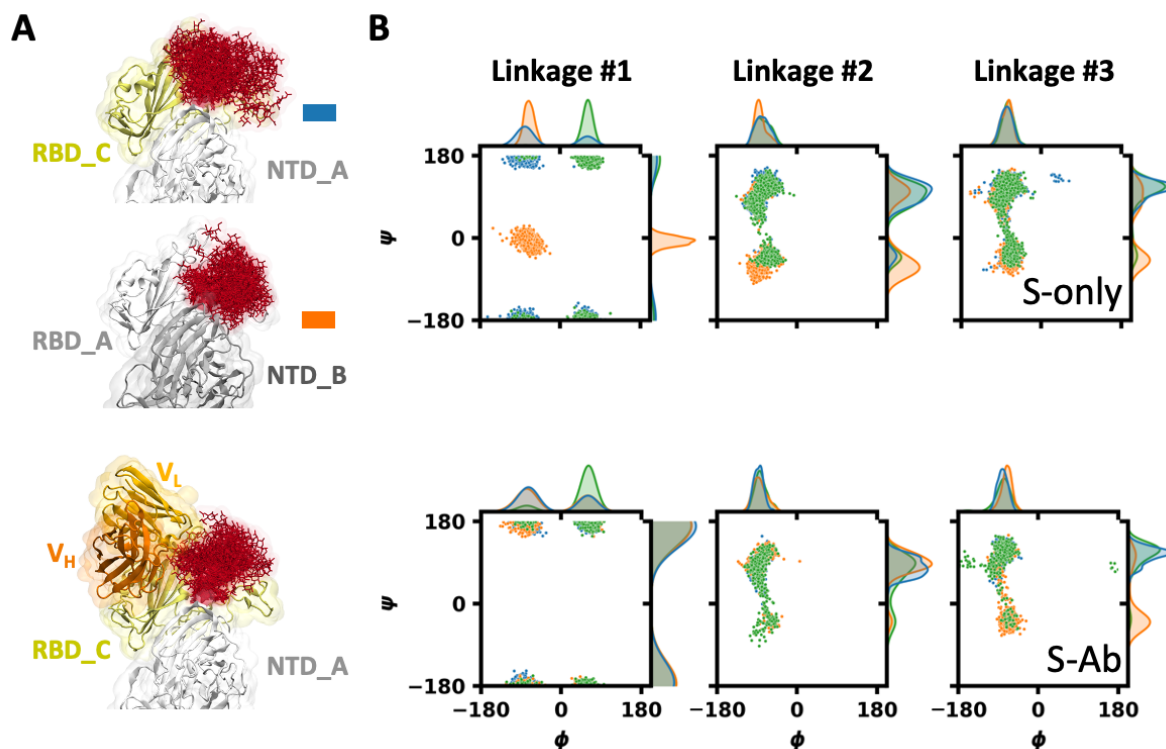


Figure S21. Glycan flexibility in S-only and S-antibody complex systems: N165 glycan in S309_CCC. (A) The structures generated by superimposing the glycan (red) onto the initial structure. (B) The distributions of ϕ/ψ angles in the first three glycosidic linkages from the reducing terminus. The glycans attached to three protomers (chains A, B, and C) are shown in blue, orange, and green, respectively. For S-only systems, we show the structures of N165 glycan attached to RBD_A (blue) and RBD_B (orange), where the glycan is sampled on two different neighbors.

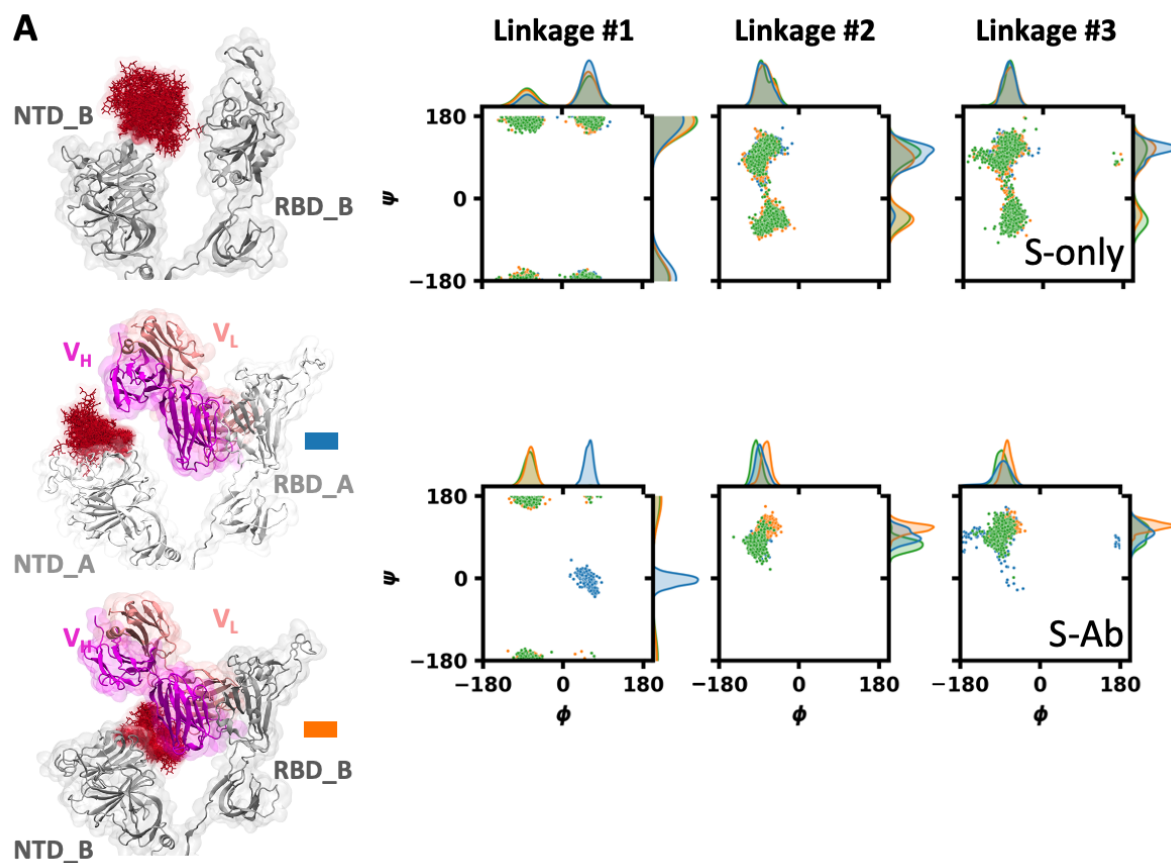


Figure S22. Glycan flexibility in S-only and S-antibody complex systems: N165 glycan in EY6A_OOO. (A) The structures generated by superimposing the glycan (red) onto the initial structure. (B) The distributions of ϕ/ψ angles in the first three glycosidic linkages from the reducing terminus. The glycans attached to three protomers (chains A, B, and C) are shown in blue, orange, and green, respectively. For S-antibody complex systems, we show the structures of N165 glycan attached to RBD_A (blue) and RBD_B (orange), where the glycan is sampled on two different neighbors.

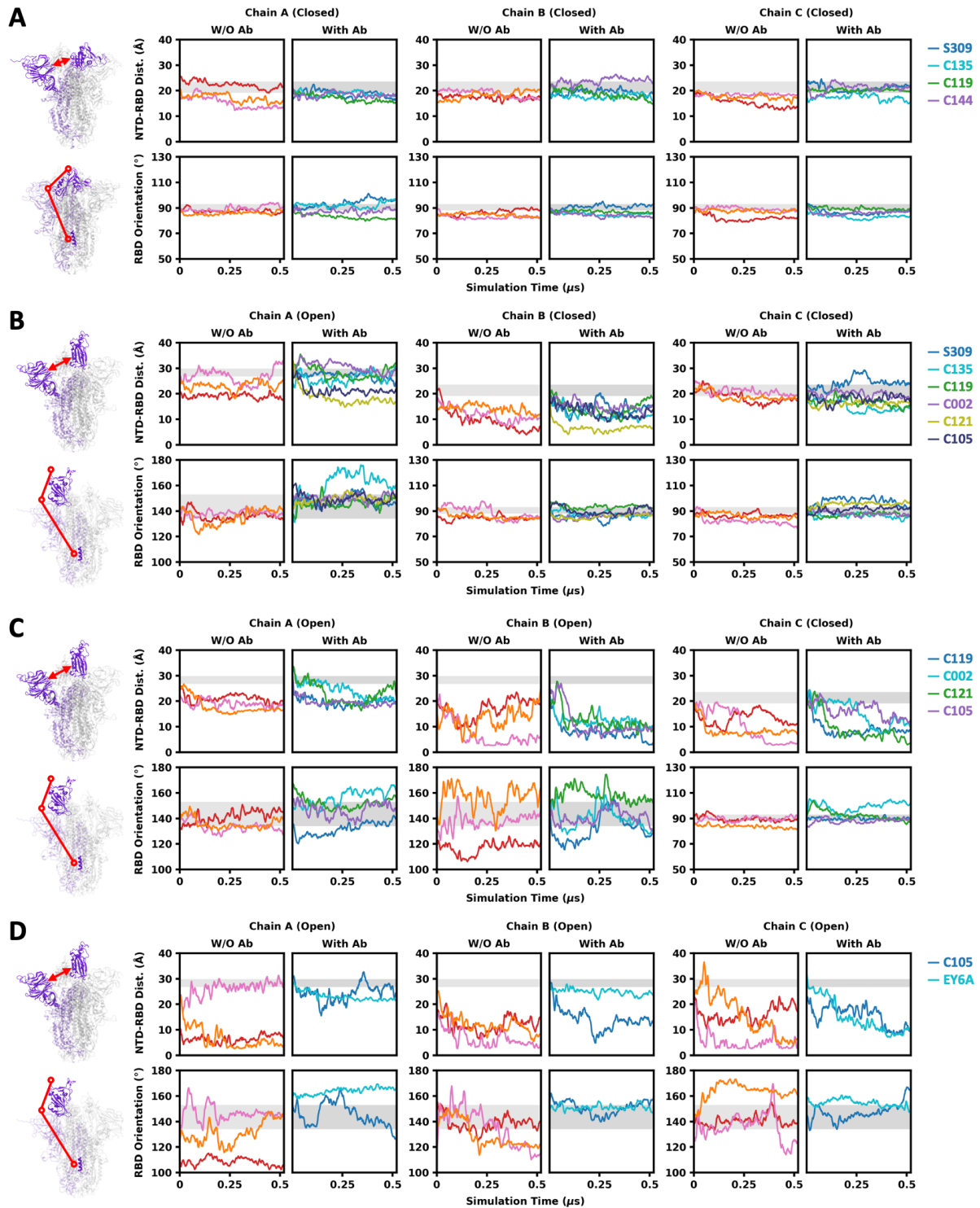


Figure S23. NTD-RBD distance (d) and RBD orientation angle (θ) in S-only and S-antibody complex systems. (A) All closed, (B) one RBD open, (C) two RBDs open, and (D) all open. Three trajectories of S-only systems are shown in red, pink, and orange. The trajectories of S protein in complex with various antibodies are shown in the colors labeled on the right. The ranges of d and θ observed in available PDB S protein structures are shaded by gray regions.

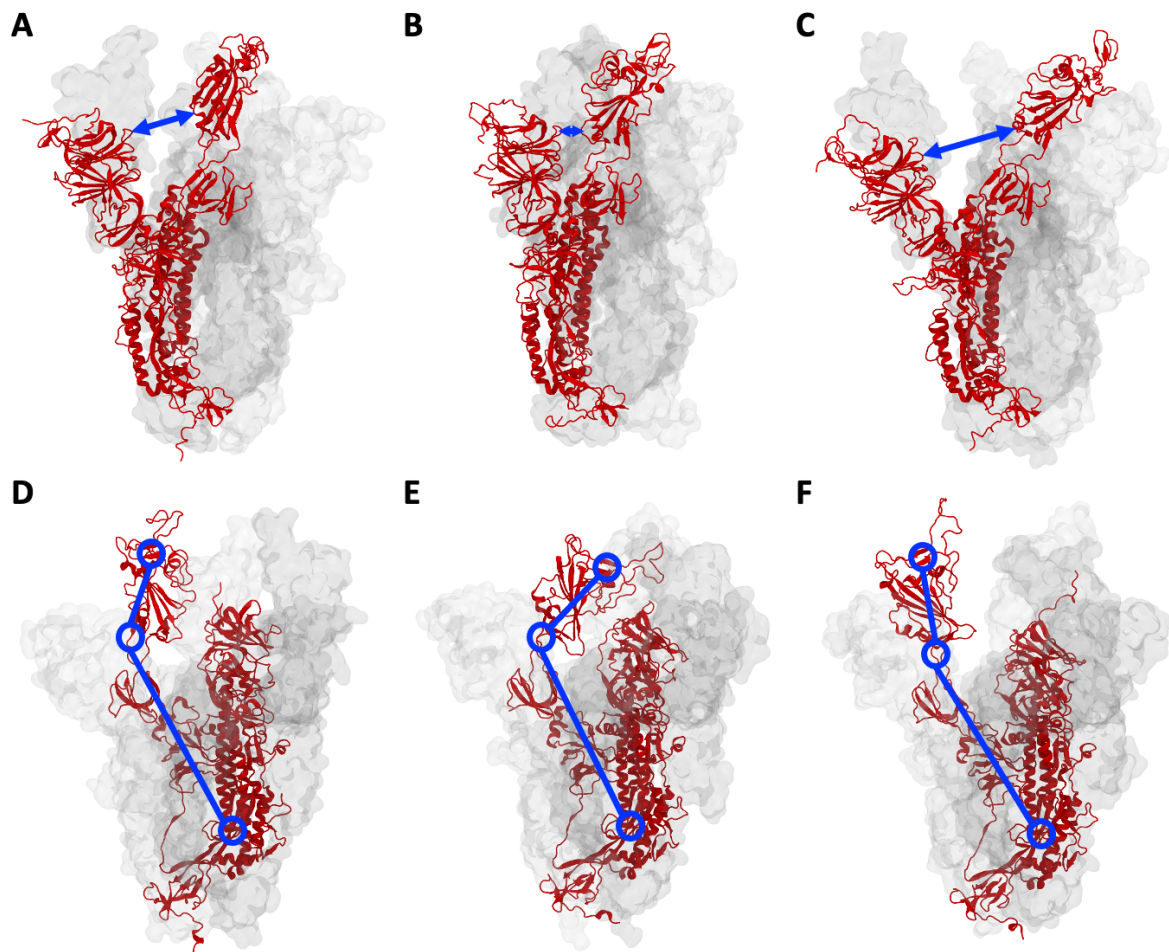


Figure S24. Representative structures with various NTD-RBD distances (d) and RBD orientation angles (θ). (A-C) NTD-RBD distance: moderate, close, and distant. (D-F) RBD orientation: open, half open, and extra open.

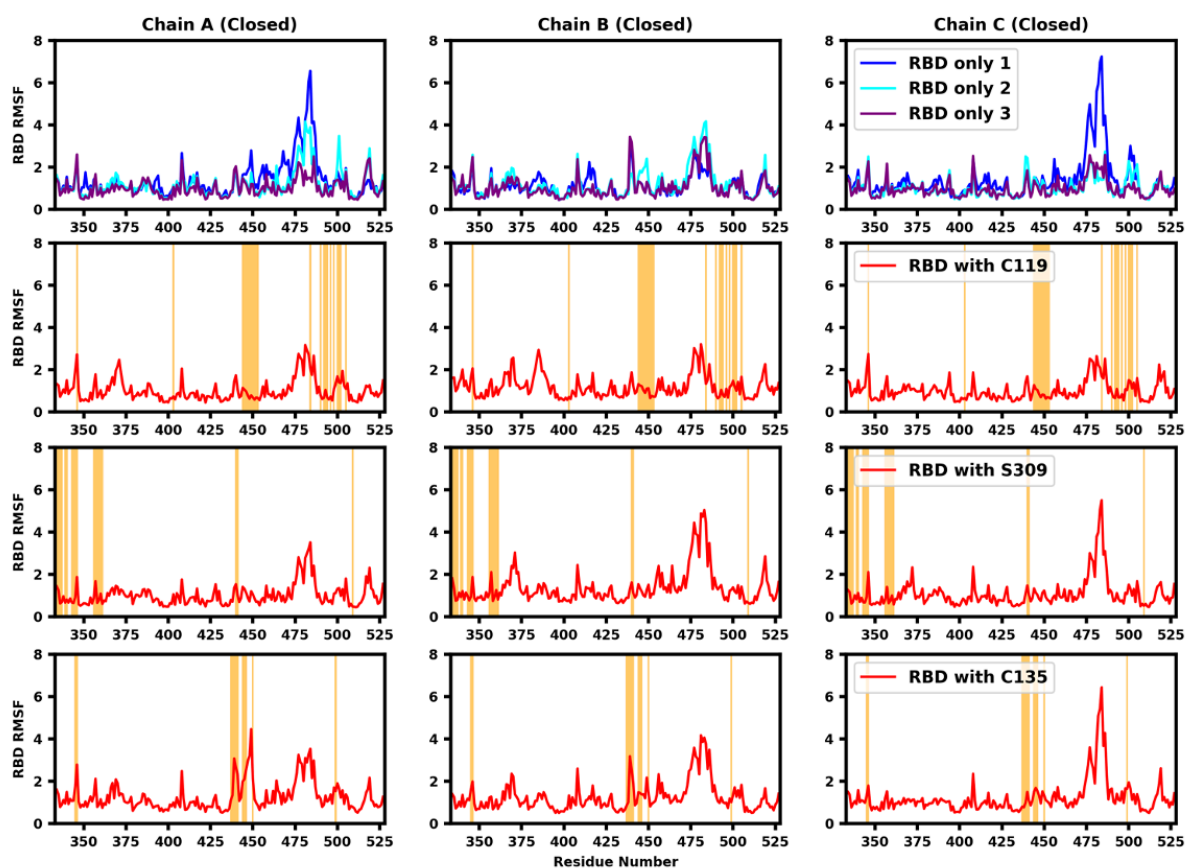


Figure S25. RMSF of RBD in S-only and S-antibody complex systems with all three RBDs closed. Three trajectories of S-only systems are shown in blue, cyan, and purple, and the trajectories of S-antibody systems are shown in red. The residues in the epitope of each antibody are shaded by orange regions.

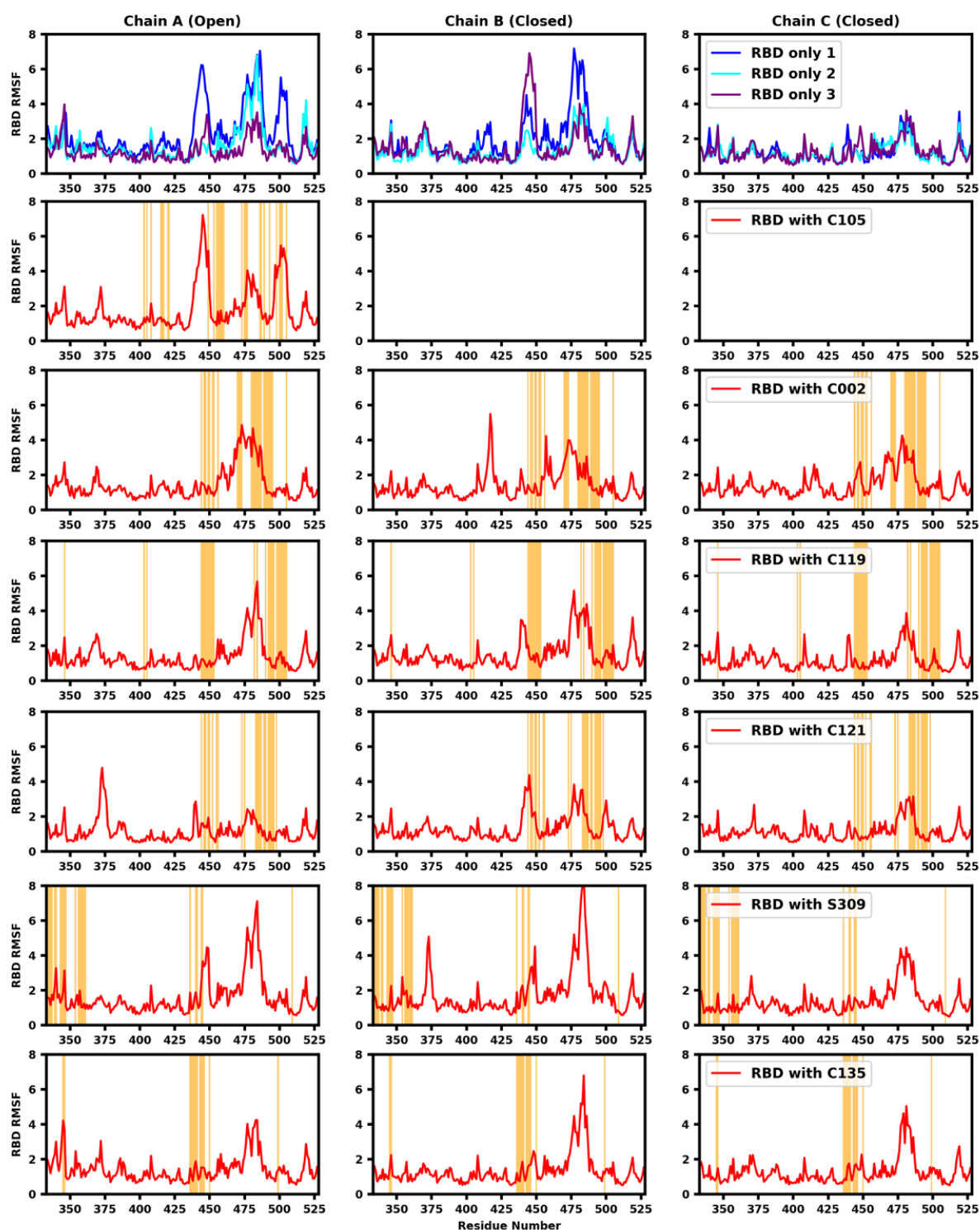


Figure S26. RMSF of RBD in S-only and S-antibody complex systems with one RBD open and two RBDs closed. Three trajectories of S-only systems are shown in blue, cyan, and purple, and the trajectories of S-antibody systems are shown in red. The residues in the epitope of each antibody are shaded by orange regions.

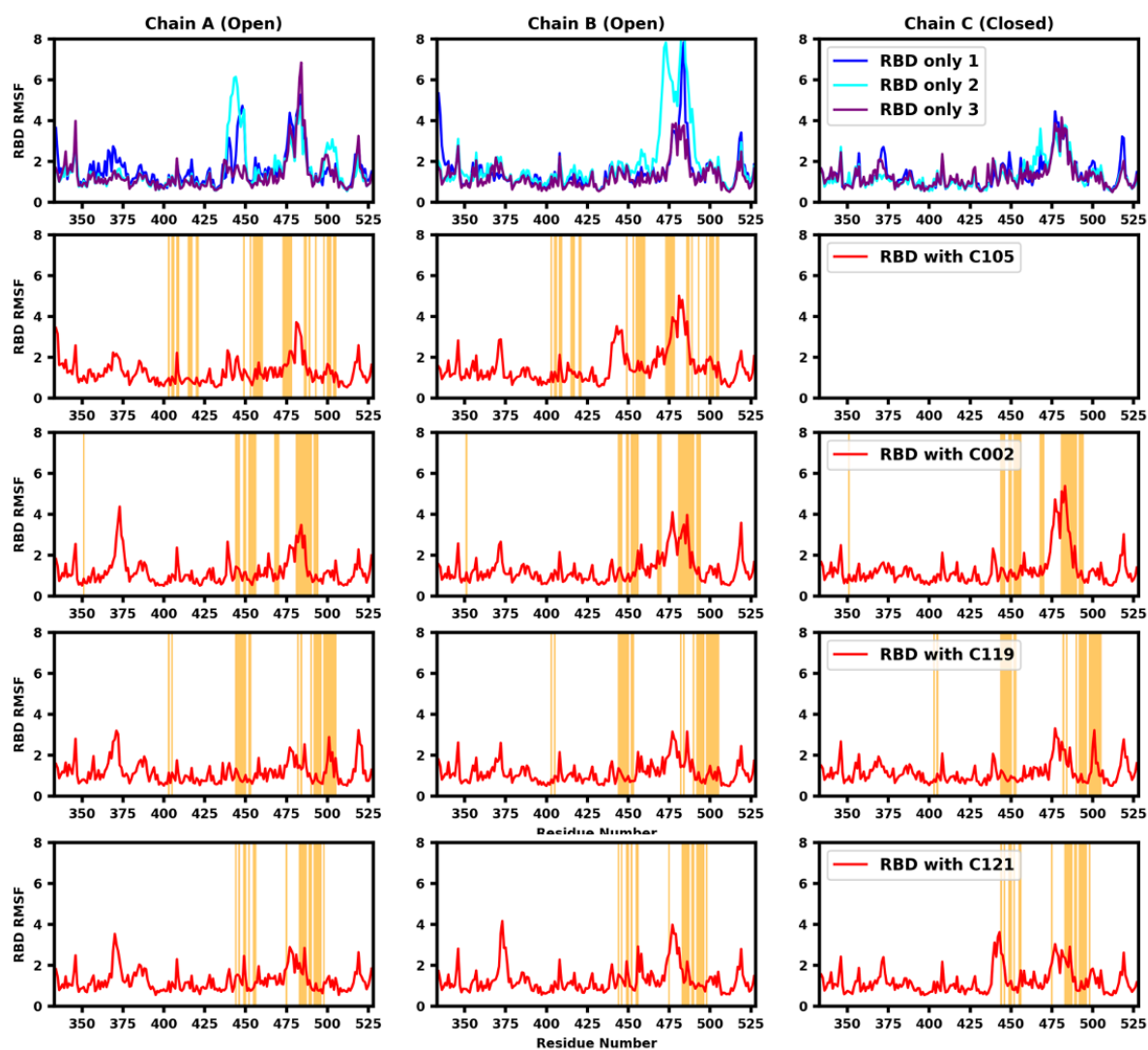


Figure S27. RMSF of RBD in S-only and S-antibody complex systems with two RBDs open and one RBD closed. Three trajectories of S-only systems are shown in blue, cyan, and purple, and the trajectories of S-antibody systems are shown in red. The residues in the epitope of each antibody are shaded by orange regions.

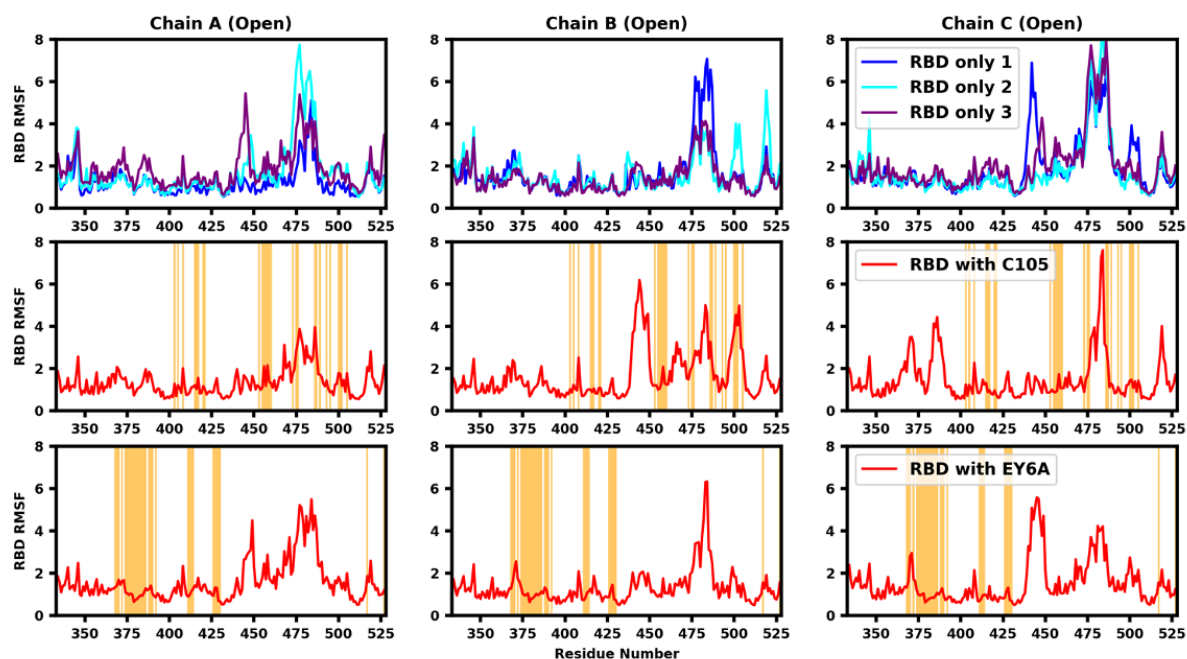


Figure S28. RMSF of RBD in S-only and S-antibody complex systems with all three RBDs open. Three trajectories of S-only systems are shown in blue, cyan, and purple, and the trajectories of S-antibody systems are shown in red. The residues in the epitope of each antibody are shaded by orange regions.